

Signal Processing Advances for 3G WCDMA: From Rake Receivers to Blind Techniques

Youngchul Sung and Yirang Lim, KAIST

Lang Tong, Cornell University

Alle-Jan van der Veen, TU Delft

ABSTRACT

As already deployed and proven technology, code-division multiple access has evolved to support competitive high-data-rate low-latency multimedia services over wireless cellular networks. In this article we introduce advanced signal processing techniques to enhance CDMA receiver performance further. In particular, we consider the possibility of optimal joint multiuser detection for long code WCDMA using fast inversion based on a state-space approach with reasonable complexity, and semi-blind channel estimation techniques to realize rate-efficient transmission for the latest 3G standards.

INTRODUCTION

Code-division multiple access (CDMA) has been playing a major role in wireless digital cellular networks since the mid-1990s. CDMA allows each user to transmit over a wideband spectrum, and provides various desirable system features such as universal frequency reuse, soft handoffs between adjacent cells, and softer handoffs between sectors of the same cell [1]. After the great success of IS-95, wideband CDMA (WCDMA) has been adopted as one of the third-generation (3G) wireless standards by the Third Generation Partnership Project (3GPP) with initial standard Releases 99 and 4. Since then, WCDMA has continuously evolved to support various applications such as wireless Internet, video telephony, and voice over IP (VoIP). For example, high-speed downlink packet access (HSDPA) was introduced to provide packet-switched connectivity in the downlink direction in Release 5 in 2002, and high-speed uplink packet access (HSUPA), also known as enhanced uplink (EUL), was introduced to support packet access in the uplink in Release 6 in 2004. These technologies accomplish low latency and reliable packet transmission using channel-adaptive high

order modulation, hybrid automatic repeat request (H-ARQ), and fast inner-loop and outer-loop power control at the physical layer, and provide peak rates of 11.4 Mb/s and 5.74 Mb/s in the downlink and uplink, respectively.

On the other hand, the fourth generation (4G) wireless standards are based primarily on orthogonal frequency-division multiple access (OFDMA). Several proposals based on OFDMA are under consideration for the 4G wireless standard for IMT-Advanced, such as mobile WiMAX, ultra mobile broadband (UMB), and 3G long term evolution (LTE). In OFDMA systems the initial latency problem¹ in the uplink (random) access in CDMA is mitigated due to the orthogonality among users. However, these systems also have other issues such as intercarrier interference at high Doppler frequency. With universal frequency reuse, most of all, cell edge users in OFDMA systems suffer intercell interference even with sophisticated bin assignment for the physical channel due to the lack of interference mitigation measures. Recently, further improvement of high-speed packet access for WCDMA was standardized in 3GPP Release 7, known as HSPA+, in June 2007. This evolution provides several enhancements in end-user performance, throughput, and network architecture, and supports peak rates of 28.8 Mb/s and 11.5 Mb/s with 5 MHz bandwidth for downlink and uplink, respectively. These rates are competitive in spectral efficiency with the peak rates of 3GPP LTE with 100 Mb/s and 50 Mb/s over 20 MHz bandwidth in downlink and uplink, respectively. The high rates of Release 7 are accomplished by employing various advanced transmission techniques, such as discontinuous uplink transmission (DTX), multi-input multi-output (MIMO) antenna, higher order modulation, and flat network architecture [2, 3].

For WCDMA to support these rates and continue being competitive, advanced signal pro-

¹ Since the CDMA uplink is quasi-orthogonal, each user ramps up its transmission power from a conservative initial value in order not to disturb the system's stability.

cessing techniques and receiver architectures are essential at physical layer. In the CDMA downlink, perfect orthogonal spreading codes such as Walsh-Hadamard codes or orthogonal variable spreading factor (OVSF) codes are used, and no interference is caused among users of the same cell in additive white Gaussian noise (AWGN) channels. In a typical wireless environment, however, the orthogonality is destroyed by multipath fading, and intracell interference between users in the same cell arises. This intracell interference can be removed effectively by restoring the channel to be like an AWGN channel, using chip-level frequency-domain equalization or time-domain equalization based on adaptive filters such as the least mean square (LMS) algorithm, which is indeed an option for 3GPP Release 7 terminals. Thus, the downlink receiver processing becomes relatively manageable, and the major challenge lies in the uplink reception.

Vast research results are available to improve the performance of the CDMA uplink over the conventional matched filter receiver [1, references therein]. For example, successive interference cancellation (SIC) with a matched filter front-end can be used to remove other user interference, which is indeed implemented in current EV-DO base station receivers. To further improve receiver performance over SIC, more sophisticated front-ends such as decorrelating or minimum mean square error (MMSE) front-ends can be considered for optimal joint decoding or information theoretically optimal MMSE-SIC receivers. However, these advanced receivers require high computational complexity, especially for long code CDMA systems. To circumvent this computational complexity, other techniques such as approximating a decorrelating front-end can be considered [4]. However, these approximating techniques are based on a weak interference assumption that is not valid when the interference is strong and spreading gain is small. In the first part of this article, based on our previous work [5–7], we introduce a fast inversion technique for large structured matrices using a state-space approach, which can be used to implement decorrelating or MMSE front-ends for optimal receiver processing with reasonable complexity. Next, we discuss a semi-blind approach to channel estimation as a possible candidate to further enhance the performance of WCDMA with no change in transmission structure and achieve highly efficient transmission.

HIGHLY EFFICIENT RECEIVER ARCHITECTURES

In the uplink, we have a multiple access channel (MAC) in which multiple users transmit their signals using pseudo-random codes. Typically, a CDMA receiver is composed of various tracking loops (e.g., frequency tracking loop and time tracking loop), and further processing units for coherent demodulation and decoding. The signal model for long code WCDMA after the removal² of major frequency offset by the frequency tracking loop and with known timing by a searcher is given by a multiuser multipath model:

$$\mathbf{y} = \mathbf{H}\mathbf{s} + \mathbf{w}, \quad (1)$$

where \mathbf{w} is typically assumed to be Gaussian noise. Note that the signal part of the received signal is decomposed into three terms: $\mathbf{7}$ is the code matrix constructed from the pseudo-random codes of users, \mathbf{H} is a block diagonal matrix containing the channel information of all users, and \mathbf{s} is the data symbol vector containing all symbols of all users. (For the detailed derivation of the model, please refer to [6].)

CONVENTIONAL APPROACHES: RAKE RECEIVERS AND INTERFERENCE CANCELLATION

The classical rake receiver is a simple matched filter to obtain a symbol estimate by regarding all other user signals as interference. To illustrate this, consider the demodulation of the m th symbol of user i . The matched filtering can be accomplished in two steps. First, we multiply \mathbf{T}_{im}^H to \mathbf{y} from the left, where \mathbf{T}_{im}^H is the portion of $\mathbf{7}$ corresponding to the m th symbol of user i , and subsequently multiply a finite impulse response (FIR) channel vector estimate $\hat{\mathbf{h}}_i^H$ from the left to produce the maximal ratio combining for symbol estimate, where $(\cdot)^H$ is the Hermitian transpose. This operation can be implemented efficiently by using rake fingers (which operate on each path separately) and combining the finger outputs, and constitutes the basic algorithm for early CDMA receivers [1]. However, the rake receiver treats all other user signals as interference, and cannot achieve the MAC channel capacity. To address this problem, uplink interference cancellation for CDMA was first proposed in [8], and vast research has been conducted in multiuser detection (MUD), which is jointly optimal for decoding simultaneous user signals [9]. The sum rate capacity can be achieved theoretically using successive interference cancellation for synchronous systems with equal rate users and exponential power distribution [8], and for asynchronous systems with equal power distribution [10]. Implementations of the interference cancellation were introduced for frame-asynchronous EV-DO systems with HARQ and possibly for 3GPP Release 6 HSUPA in [11]. Indeed, the pilot channel is cancelled in EV-DO Rev.A base station modem CSM6800, and overhead and traffic channels can be cancelled further with more processing power.

In receivers with interference cancellation, typically, unknown data is first decoded using a rake receiver, reconstructed (i.e., re-encoded and filtered by the composite transmit-receive pulse shaping response using further information about timing, carrier offset, and channel coefficients), and subtracted from the received signal sample buffer, and the next packets are fetched from the sample buffer and decoded. Even if interference cancellation can achieve the sum rate capacity ideally, this is not the case in real situations. The practical performance of interference cancellation depends on the success in decoding the previous packets, the decoding order, and the quality of signal reconstruction. Here, a channel estimate is required for signal reconstruction, and the channel estimate may

Even if the interference cancellation can achieve the sum rate capacity ideally, this is not the case in real situations. The practical performance of the interference cancellation depends on the success of decoding of the previous packets, the decoding order and the quality of signal reconstruction.

² At this point the block fading assumption holds for the data model.

The key idea for fast inversion is to replace the code matrix multiplication by filtering through a time-varying state-space linear system and to implement the inversion locally in state space.

not be accurate, especially when the pilot channel operates in low signal-to-noise ratio (SNR) and the traffic-to-pilot power ratio is not large as in VoIP applications.

MULTIUSER DETECTION FOR LONG CODE WCDMA: SYSTEM-THEORETIC APPROACH

The optimal processing of Eq. 1 is given by the joint maximum likelihood (ML) decoding or MUD that detects all users' symbols simultaneously [9], and thus there remains a room for further performance improvement by MUD over the suboptimal interference cancellation [12]. Most research in MUD has been performed for short-code cases [9]. In practice, however, most systems adopt long code CDMA for various reasons. The MUD is based on the inversion of the code matrix, i.e., decorrelation (or zero-forcing) \tilde{T}^\dagger or MMSE inversion $(\tilde{T}^H\tilde{T} + \sigma^2\mathbf{I})^{-1}\tilde{T}^H$, where \tilde{T}^\dagger is the Moore-Penrose pseudo-inverse of \tilde{T} and \mathbf{I} is an identity matrix. Consider a WCDMA system with 40 users with lowest data rate (i.e., spreading gain $G = 256$) in a sector. The signal processing is performed based on a 2 ms transmission time interval (TTI) that consists of three slots with 7680 chips. Incorporating three multipaths per user, the size of the code matrix \tilde{T} in Eq. 1 is given by 7680×3600 . The inversion of such a large code matrix within 2 ms is a very challenging task. Fortunately, the code matrix is highly structured and sparse; only 3.3 percent of the elements are nonzero for the above example. The simple inversion of the code matrix will lose the sparse structure. Therefore, the sparsity and structure should be exploited to accomplish fast inversion. In this section we introduce the theory and algorithms developed by Dewilde and van der Veen [5, 6] for the fast inversion of large structured matrices based on linear system theory, which can be used for an efficient realization of MUD for long code CDMA.

Linear Time-Varying Equivalent System and Fast Inversion

Equivalent State-Space Realization — The key idea for fast inversion is to replace the code matrix multiplication by filtering through a time-varying state-space linear system and to implement the inversion locally in state space. That is, we have two equivalent systems:

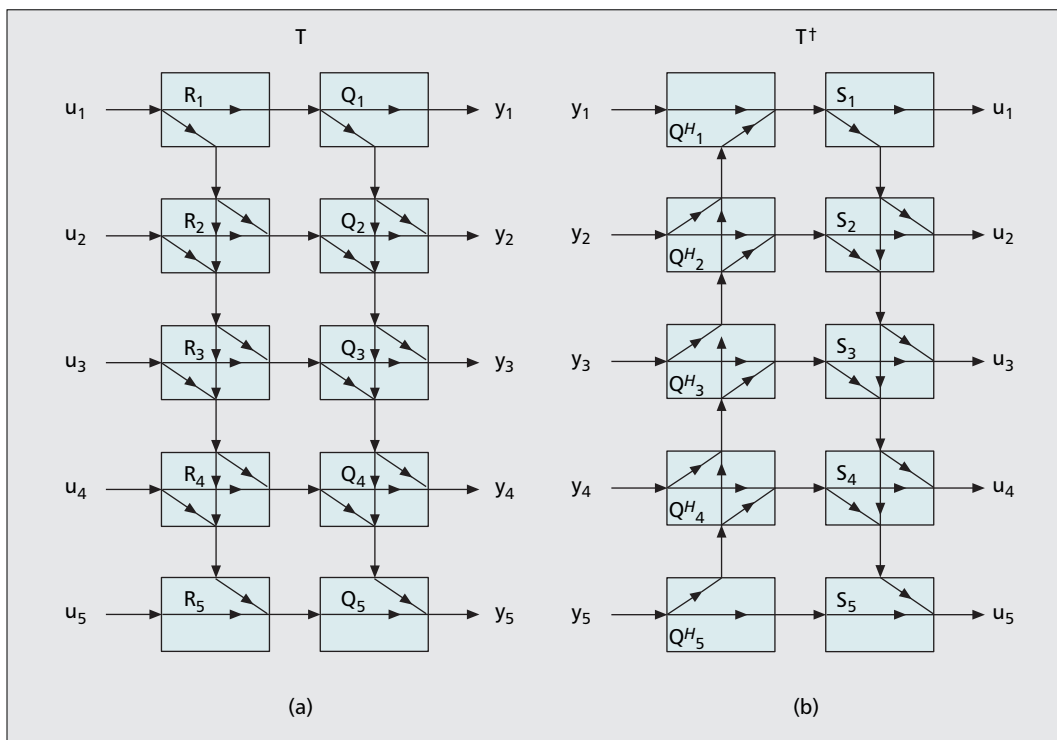
$$\begin{aligned} \text{matrix multiplication} & : \quad y \triangleq \begin{bmatrix} y_1 \\ \vdots \\ y_N \end{bmatrix} = \tilde{T}\mathbf{u}, \\ \text{state-space equivalent} & : \quad \begin{bmatrix} \mathbf{x}_{n+1} \\ y_n \end{bmatrix} \\ & = \begin{bmatrix} \mathbf{A}_n & \mathbf{B}_n \\ \mathbf{C}_n & \mathbf{D}_n \end{bmatrix} \begin{bmatrix} \mathbf{x}_n \\ \mathbf{u}_n \end{bmatrix} \end{aligned} \quad (2)$$

where $\{\mathbf{A}_n, \mathbf{B}_n, \mathbf{C}_n, \mathbf{D}_n\}_{n=1}^N$ and $\{\mathbf{u}_n\}_{n=1}^N$ are properly constructed from the code matrix \tilde{T} in Eq. 1 and the input vector \mathbf{u} so that the output $\{y_n\}_{n=1}^N$ is the same for the two systems for time $n = 1,$

$2, \dots, N$. To illustrate this, we consider the matrix-vector multiplication with a simple $N \times L$ matrix \tilde{T} with rows \mathbf{t}_n^H and a $L \times 1$ input vector \mathbf{u} . Here, we have $y_n = \mathbf{t}_n^H \mathbf{u}$. The equivalent state-space representation for this system is given by setting $\mathbf{u}_1 = \mathbf{u}, \mathbf{u}_2 = \dots = \mathbf{u}_N = \bullet$ and $\{\mathbf{A}_1, \mathbf{B}_1, \mathbf{C}_1, \mathbf{D}_1\} = \{\bullet, \mathbf{I}, \bullet, \mathbf{t}_1^H\}, \{\mathbf{A}_n, \mathbf{B}_n, \mathbf{C}_n, \mathbf{D}_n\} = \{\mathbf{I}, \bullet, \mathbf{t}_n^H, \bullet\}$ for $n = 2, \dots, N-1$ and $\{\mathbf{A}_N, \mathbf{B}_N, \mathbf{C}_N, \mathbf{D}_N\} = \{\bullet, \bullet, \mathbf{t}_N^H, \bullet\}$. It is easy to verify that this state-space representation yields the same output as the original matrix-vector multiplication by defining the product of the empty element \bullet and a matrix (or vector) as an empty element again. For more complicated matrices, including the full code matrix \tilde{T} in Eq. 1, it is also easy to construct equivalent state-space representations. For \tilde{T} , in particular, we can choose N to be the number of rows of \tilde{T} , and the input vector is properly partitioned and applied to the system at appropriate time instants. Here, the dimension of the state at time n is typically the number of nonzero elements in the n th row of \tilde{T} .

Inversion in State Space — Once state-space realization $\{\mathbf{A}_n, \mathbf{B}_n, \mathbf{C}_n, \mathbf{D}_n\}_{n=1}^N$ and $\{\mathbf{u}_n\}_{n=1}^N$ are available, the inversion can be done by inverse filtering in state space. As in many other cases, stable inversion can be implemented via QR factorization even in state space. First, note that the code matrix multiplication can be done in two steps using QR factorization: $\mathbf{u} \xrightarrow{\mathbf{R}} \mathbf{z} \xrightarrow{\mathbf{Q}} \mathbf{y}$. The state-space realization of each of \mathbf{Q} and \mathbf{R} factors of \tilde{T} can be obtained from $\{\mathbf{A}_n, \mathbf{B}_n, \mathbf{C}_n, \mathbf{D}_n\}_{n=1}^N$. It is shown in [6] that the state-space realization $\{\mathbf{A}_n^Q, \mathbf{B}_n^Q, \mathbf{C}_n^Q, \mathbf{D}_n^Q\}_{n=1}^N$ of the \mathbf{Q} factor and $\{\mathbf{A}_n^R, \mathbf{B}_n^R, \mathbf{C}_n^R, \mathbf{D}_n^R\}_{n=1}^N$ of the \mathbf{R} factor can be obtained by simple recursion. The overall QR system via state-space realization is shown in Fig. 1a. Based on the state-space QR realization, the inversion system is now realized in state space easily. First we apply the inversion to the \mathbf{Q} system and then to the \mathbf{R} system. Since \mathbf{Q}_n satisfies $\mathbf{Q}_n^H \mathbf{Q}_n = \mathbf{I}$, the first inversion is straightforward. The inversion for the second \mathbf{R} system can be implemented by changing the input-output relationship. That is, from the state space representation $\{\mathbf{A}_n^R, \mathbf{B}_n^R, \mathbf{C}_n^R, \mathbf{D}_n^R\}_{n=1}^N$ and the linearity between input and output, the output is represented by a linear combination of the input and state, and this yields the state-space representation \mathbf{S}_n for the inverse system of \mathbf{R} . Thus, the overall inversion system is shown in Fig. 1b. Note that the inversion of the \mathbf{Q} system is anticausal. Note also that the overall inversion is accomplished by successive application of small size inversions in state space, and this is the main reason for drastic complexity reduction. The MMSE front-end can also be implemented using the state-space approach readily with slight modification [6].

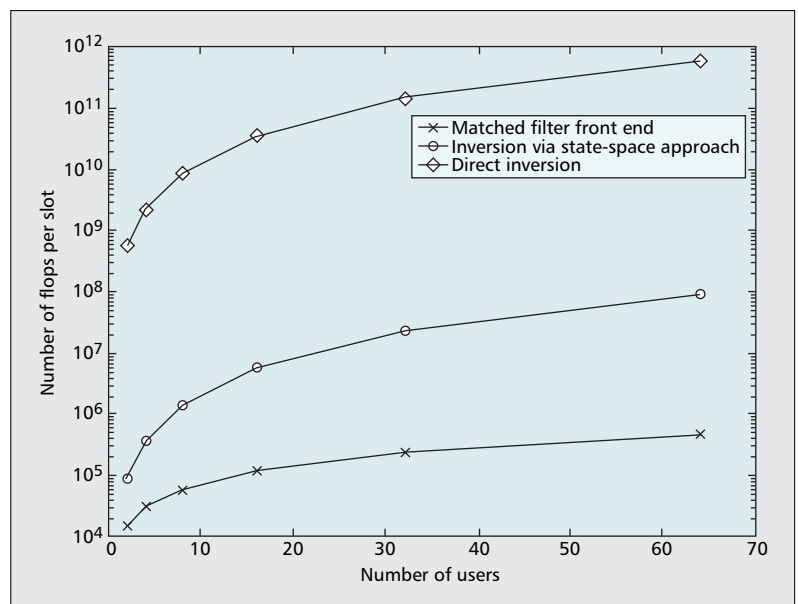
Complexity, Implementation, and Performance — To assess the complexity of the inversion using the state space approach, we consider a K user system with equal spreading gain G , block size of M symbols, and L multipaths. In this case the size of \tilde{T} is roughly $GM \times MLK$. The main complexity of the inversion using the state space approach lies in the QR recursion step. It is shown in [6] that \mathbf{A}_n and \mathbf{B}_n are either \bullet or \mathbf{I} ,



■ Figure 1. a) QR factorization in state space; b) inversion in state space [6].

$[C_n, D_n]$ has only one row, the maximum size of A_n is $2LK \times 2LK$, the maximum column size of C_n is $2LK$, and the column number of D_n is either zero or LK . Thus, the QR recursion for each n requires the QR factorization of a $2LK \times 2LK$ matrix, which requires complexity in order of $O(L^2K^2)$. Since we have GM time steps, the overall complexity is given by $O(GM(LK)^2)$. On the other hand, the direction inversion based on normal equation will result in complexity of $O(GM^3(LK)^2)$, and applying the matched filter has complexity of the order of non-zero elements in T , that is, $O(GMLK)$. Thus, inversion based on the state-space approach reduces the complexity by an order of magnitude compared to direct inversion, and both the matched filter and state-space approaches have complexity linear with respect to the number of chips per slot. Figure 2 shows the number of flops per slot with respect to the number of users in the system with parameters $G = 32$, $M = 80$, $L = 3$, and 2560 chips/slot, and Fig. 3 shows a possible implementation for the inversion algorithm.

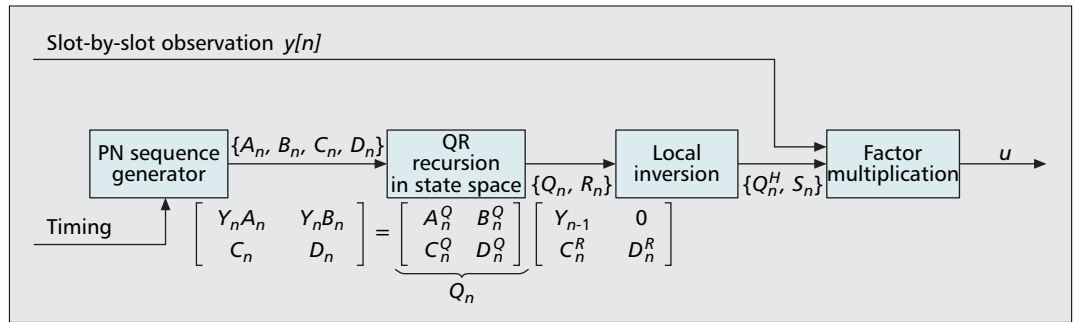
Since the left inverse T^\dagger requires the matrix to have full column rank, the code matrix T may not include all users in the system. (This is the case for any decorrelating or MMSE front-ends.) In such cases MUD based on inversion can be used jointly with interference cancellation, where strong and important user signals are processed using MUD after the interference from the remaining users is subtracted using interference cancellation. Several more issues such as timing and chip-level fractional sampling should be considered for such algorithms to be used in practice. Fast inversion based on the state-space approach can also be used in the downlink. In HSDPA, for example, cell edge users receive signals from two base stations, and equalizing the



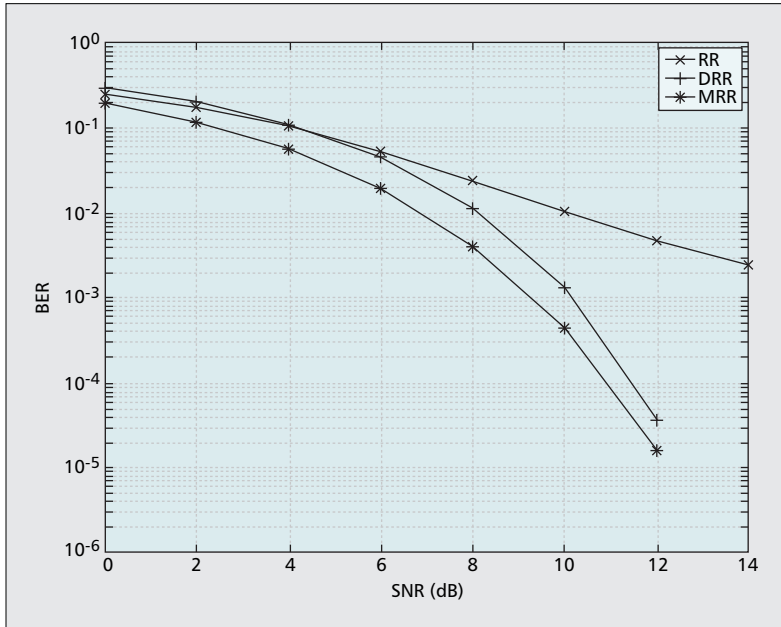
■ Figure 2. Computational complexity of various receivers.

signal according to one base station cannot properly remove the interference from the other cell. In this case decorrelating or MMSE inversion based on the fast algorithm can provide the optimal joint decoding.

Figure 4 shows the performance of receivers with different front-end processing. We considered three front-ends — conventional match filter, decorrelating front-end, and MMSE front-end — to see the impact of different front-end processing. For simplicity, we used the same post-processing of a rake multipath combiner.



■ **Figure 3.** An implementation of long code MUD based on the state-space approach.



■ **Figure 4.** BER performance of various receivers: RR: rake receiver with matched filter front-end, DRR: rake receiver with decorrelating front-end, MRR: rake receiver with MMSE front-end ($G = 32$, $M = 80$, and 5 asynchronous users [$K = 5$]).

As expected, the performance of the matched-filter-based receiver deteriorates as the SNR increases since it cannot remove other user interference effectively. On the other hand, receivers with inversion-based front-end processing show the desired waterfall bit error rate (BER) behavior. Note that there is a performance gain of almost 1 dB by the MMSE front-end over the decorrelating front-end in this case. When more advanced receivers like MMSE-SIC are adopted, the performance gain is expected to become larger.

RATE-EFFICIENT CHANNEL ESTIMATION: SEMI-BLIND APPROACHES

In the previous section we introduce an efficient inversion technique based on the state-space approach that can be used for advanced long code WCDMA receivers such as MUD and MMSE-SIC to improve receiver performance.

³ This is typically the case for large transport block size.

Another improvement for WCDMA can be attained using semi-blind channel estimation techniques that exploit unknown data as well as known pilot symbols. These techniques are especially worth considering for 3GPP Release 7 in which higher order modulations, such as 64-quadrature amplitude modulation (QAM) for downlink and 16-QAM for uplink, are adopted, and the importance of channel estimation is emphasized. Furthermore, terminals completely shut down transmission (even including the transmission of pilot channel) to save battery when there is no data to transmit. Thus, it is indeed desirable to use all available signal for channel estimation during transmission. There is vast literature in the area of blind and semi-blind channel estimation for CDMA systems (e.g., [13]). In this section we consider one example of semi-blind channel estimation techniques suited to WCDMA data structure [14], and show the benefit of semi-blind techniques that use both unknown data and pilot symbols for channel estimation.

The WCDMA uplink physical layer has two code channels: a dedicated physical control channel (DPCCH) and a dedicated physical data channel (DPDCH). The DPCCH carries known pilot symbols and control bits, while the DPDCH is the payload containing unknown data symbols. Typically, the pilot-based channel estimation for WCDMA first calculates the slot average, and several slot averages are combined with proper weighting to yield a channel estimate for the current slot period [15]. However, this conventional method uses only known pilot symbols, and unknown data from the same user (as well as other user signals) acts as interference to channel estimation. In the context of interference cancellation, an iterative channel estimation method can be used [10]. That is, when the traffic-to-pilot power ratio is large³ and the decoding of data using the pilot-based channel estimate is successful, we can re-estimate the channel using the known data to yield a better channel estimate that can be used for signal reconstruction for interference cancellation. For the first decoding, however, the traffic channel with large traffic-to-pilot power ratio results in interference to channel estimation based on the pilot channel in a multipath environment. For applications like VoIP, in addition, the traffic-to-pilot power ratio is not as high, and the iterative approach is not as attractive. Thus, it is desirable to use the unknown data simultaneously with the

pilot symbols to produce a better channel estimate. The signal model incorporating both pilot and data is given by

$$\begin{aligned} \mathbf{y} &= \mathbf{T}_p(\mathbf{I}_M \otimes \mathbf{h})\mathbf{s}_p + \mathbf{T}_d(\mathbf{I}_M \otimes \mathbf{h})\mathbf{s}_d + \mathbf{w}, \\ &= \mathbf{H}(\mathbf{s}_p)\mathbf{h} + \mathbf{T}_d(\mathbf{I}_M \otimes \mathbf{h})\mathbf{s}_d + \mathbf{w}, \end{aligned} \quad (3)$$

where \mathbf{T}_p and \mathbf{T}_d are the code matrices composed of pilot spreading code and data spreading code, respectively, \mathbf{h} is the $L \times 1$ FIR channel vector, \mathbf{s}_p and \mathbf{s}_d are vectors containing pilot symbols and data symbols, respectively, \mathbf{I}_M is an identity matrix with size M , and \otimes is the Kronecker product. For the first term in the right-hand side of the second equation, the filtering form is rewritten in the data matrix form using the linearity of the channel and knowledge of the pilot symbols. The maximum likelihood estimation (MLE) for \mathbf{h} based on the pilot is given by the least square solution under the AWGN assumption, which is further simplified to the conventional pilot filter by assuming large spreading gain. In this case each channel tap coefficient is estimated simply by the correlation between the received signal and the pseudo-random code. For this method, however, the self-interference from the pilot channel and data channel is caused for each tap estimate by multipath fading.

There are several ways to use the unknown data in the above equation simultaneously for channel estimation. We introduce a semi-blind method based on projection from [14]. Note that the signal subspace of the data part in Eq. 3 is still known even if the data symbols are unknown, and the basis of the signal subspace is given by the columns of \mathbf{T}_d . Thus, the interference from unknown data can effectively be removed by projecting the received signal onto a proper subspace. This can be achieved by either orthogonal or oblique projection. Orthogonal projection projects the received signal \mathbf{y} onto the orthogonal space of the data signal subspace \mathbf{T}_d , while oblique projection projects \mathbf{y} along with the subspace of \mathbf{T}_d yielding $\mathbf{H}(\mathbf{s}_p)\mathbf{h}$ as the projection image. Figure 5 shows the relationship between the corresponding subspaces. Once projection is applied, the channel can then be estimated using several methods such as an MLE or MMSE estimator. For an example of orthogonal projection \mathbf{P} with $\mathbf{P}\mathbf{T}_d = \mathbf{0}$, the projected signal $\mathbf{P}\mathbf{y}$ does not have interference from the DPDCH. Based on the projected signal, the MLE or MMSE estimate of \mathbf{h} can be obtained.

Figure 6 shows the performance of semi-blind estimation based on orthogonal projection. Here, the traffic-to-pilot power ratio is set to 3 dB, the number of pilot symbols is four, and the number of channel taps is three. It is shown that the semi-blind method achieves the Cramér-Rao bound (CRB) for unbiased estimators, and outperforms the pilot-based estimation at intermediate and high SNR, and the gain increases as the SNR increases further. This is because at high SNR the data channel introduces self-interference due to multipath fading, and the performance is limited by this interference. Note that the MMSE estimation combined with the semi-blind technique shows desirable performance; at

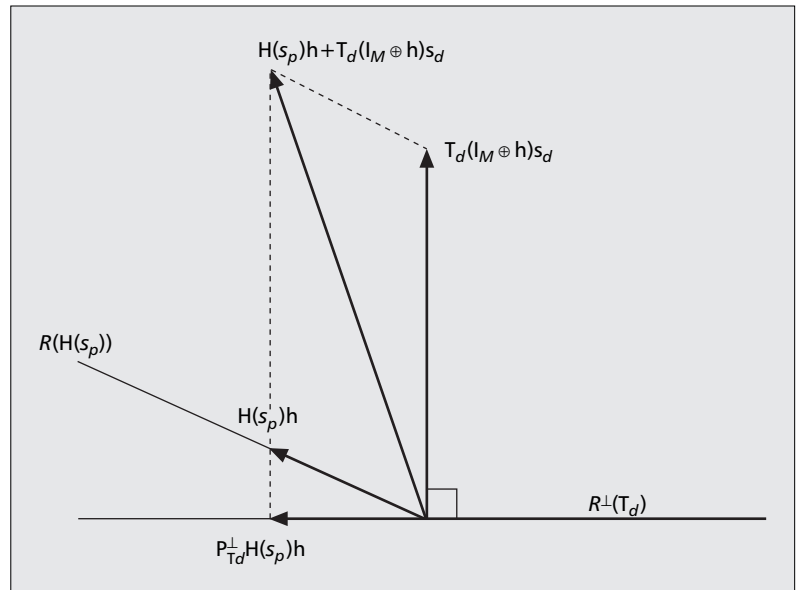


Figure 5. Projection-based semi-blind estimation: signal space decomposition.

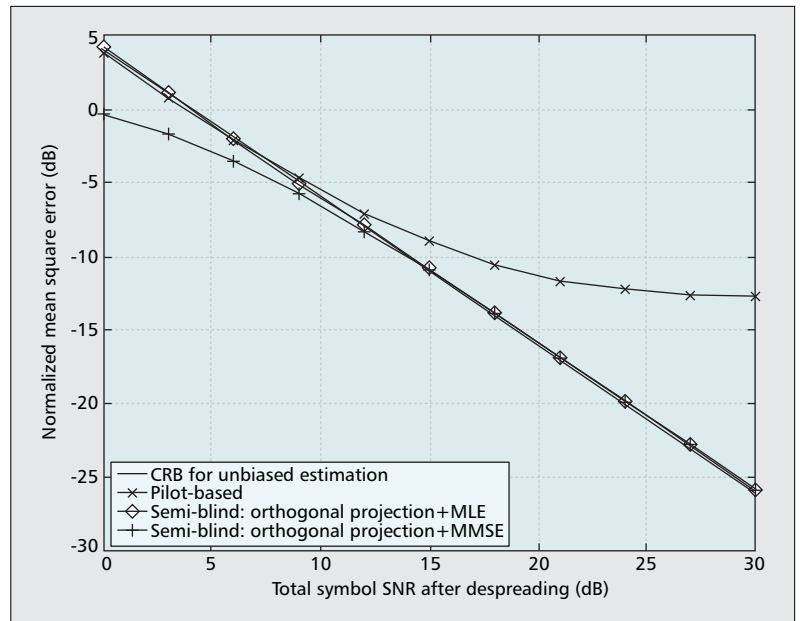


Figure 6. Projection-based semi-blind estimation: performance.

low SNR a performance gain is obtained by suppressing noise enhancement by the MMSE method, and at high SNR interference from the DPDCH is effectively removed by the semi-blind technique. (Note also that MMSE-based semi-blind estimation outperforms the CRB for unbiased estimators at low SNR. This is because MMSE-based estimation is not unbiased.) Considering that operating normalized MSE is less than -10 dB (even lower for higher order modulation), significant gain can be obtained from semi-blind estimation techniques as illustrated in this example.

Semi-blind channel estimation methods would require more complexity than conventional pilot-based approaches. However, these methods can be implemented efficiently too. For our example

With exponentially increasing processing power, challenging receiver algorithms such as optimal MUD and semi-blind channel estimation are worth considering for implementation.

of the orthogonal-projection-based semi-blind method, orthogonal projection can be implemented efficiently using the state-space inversion in the previous section since it involves the inversion of the code matrix \mathbf{T}_d , which is a sparse matrix. The interference from other user signals can also be effectively removed by interference cancellation or joint MUD described in the previous section.

CONCLUSION

In this article we have considered several advanced signal processing techniques to improve the receiver performance further for WCDMA systems. With exponentially increasing processing power, challenging receiver algorithms such as optimal MUD and semi-blind channel estimation are worth considering for implementation. Even though fast inversion based on the state-space approach is tailored to CDMA MUD here, the algorithm can be used for many other applications requiring inversion of large structured matrices. Also, semi-blind estimation techniques can find use in many other communication receiver designs to provide rate-efficient transmission.

ACKNOWLEDGMENTS

The work of Y. Sung and Y. Lim was supported by the Ministry of Knowledge Economy (MKE)/Institute for Information Technology Advancement (IITA).

REFERENCES

- [1] A. J. Viterbi, *CDMA: Principles of Spread Spectrum Communication*, Addison-Wesley, 1995.
- [2] H. Holma et al., "High-speed Packet Access Evolution in 3GPP Release 7," *IEEE Commun. Mag.*, vol. 45, no. 12, Dec. 2007, pp. 29–35.
- [3] H. Holma and A. Toskala, *WCDMA for UMTS: HSPA Evolution and LTE*, 4th ed., Wiley, 2007.
- [4] N. Mandayam and S. Verdu, "Analysis of an Approximate Decorrelating Detector," *Proc. 33rd Annual Allerton Conf. Commun., Control, and Comp.*, vol. 5, Oct. 1995, pp. 1042–53.
- [5] P. Dewilde and A.-J. van der Veen, *Time-Varying Systems and Computations*, Dordrecht, Kluwer, 1998.
- [6] L. Tong et al., "Blind Decorrelating Rake Receivers for Long Code WCDMA," *IEEE Trans. Sig. Processing*, vol. 51, no. 6, June. 2003, pp. 1642–55.
- [7] H. Q. Dang and A.-J. van der Veen, "A Low-Complexity Blind Multi-User Receiver for Long-Code CDMA," *Eurasip J. Wireless Commun. Net.*, no. 1, Aug. 2004, pp. 113–22.
- [8] A. J. Viterbi, "Very Low Rate Convolutional Codes for Maximum Theoretical Performance of Spread-Spectrum Multiple-Access Channels," *IEEE JSAC*, vol. 8, no. 4, May 1990, pp. 641–49.

- [9] S. Verdu, *Multuser Detection*, Cambridge Univ. Press, 1998.
- [10] J. E. Smees, J. Hou, and J. B. Soriaga, "Receiver Architectures and Design Trade-Offs for CDMA Interference Cancellation," *Proc. ACSSC*, Oct. 2006, pp. 2167–71.
- [11] J. Hou et al., "Implementing Interference Cancellation to Increase the EV-DO Rev A Reverse Link Capacity," *IEEE Commun. Mag.*, vol. 44, no. 2, Feb. 2006, pp. 58–64.
- [12] A. Duel-Hallen, J. Holtzman, and Z. Zvonar, "Multuser Detection for CDMA Systems," *IEEE Pers. Commun.*, vol. 2, no. 2, Apr. 1995, pp. 46–58.
- [13] Z. Xu and M. K. Tsatsanis, "Blind Channel Estimation For Long Code Multuser CDMA Systems," *IEEE Trans. Sig. Processing*, vol. 48, no. 4, Apr. 2000, pp. 988–1001.
- [14] Y. Sung and L. Tong, "A Projection-Based Semi-Blind Channel Estimation for Long-Code WCDMA," *Proc. ICASSP*, vol. 3, no. 3, May 2002, pp. 2245–48.
- [15] H. Andoh, M. Sawahashi, and F. Adachi, "Channel Estimation Filter Using Time-Multiplexed Pilot Channel for Coherent RAKE Combining in DS-SS Mobile Radio," *IEICE Trans. Commun.*, vol. E81-B, no. 7, July 1998, pp. 1517–26.

BIOGRAPHIES

YOUNGCHUL SUNG [S'92, M'95] (ysung@ee.kaist.ac.kr) is an assistant professor in the Department of Electrical Engineering at the Korea Advanced Institute of Science and Technology (KAIST), Daejeon, Korea. He received B.S. and M.S. degrees from Seoul National University, Korea, in electronics engineering in 1993 and 1995, respectively, and a Ph.D. degree in electrical and computer engineering from Cornell University, Ithaca, New York, in 2005. From 2005 until 2007 he worked as a senior engineer in the Corporate R&D Center of Qualcomm, Inc. San Diego, California, and contributed to 3GPP Release 7.

YIRANG LIM [S'08] (imerang@kaist.ac.kr) received a B.S. degree from the Department of Electrical Engineering of KAIST in 2008. She is currently with the Wireless Information Systems Research Laboratory of the Department of Electrical Engineering, KAIST. Her research interests include statistical signal processing and information processing on graphs and large networks.

LANG TONG [S'87, M'91, SM'01, F'05] (ltong@ece.cornell.edu) is the Irwin and Joan Jacobs Professor in Engineering at Cornell University. He received a B.E. degree from Tsinghua University, Beijing, China, in 1985, and M.S. and Ph.D. degrees in electrical engineering in 1987 and 1991, respectively, from the University of Notre Dame, Indiana. He was a postdoctoral research affiliate at the Information Systems Laboratory, Stanford University in 1991. He was also the 2001 Cor Wit Visiting Professor at Delft University of Technology (TU Delft) and a visiting professor at the University of California at Berkeley in 2008.

ALLE-JAN VAN DER VEEN [F'05] (allejan@cobalt.et.tudelft.nl) received a Ph.D. degree (cum laude) from TU Delft in 1993. At present, he is a full professor in signal processing at TU Delft. He is the recipient of 1994 and 1997 IEEE Signal Processing Society (SPS) Young Author paper awards. He was Chairman of the IEEE SPS Signal Processing for Communications Technical Committee (2002–2004), Editor-in-Chief of *IEEE Signal Processing Letters* (2002–2005), Editor-in-Chief of *IEEE Transactions on Signal Processing* (2006–2008), and a member-at-large of the Board of Governors of IEEE SPS (2006–2008).